J.I. Collar[a,b] and Y. Giomataris [c]

[a] *Groupe de Physique des Solides (UMR CNRS 75-88), Universités Paris 7 & 6, 75251 Paris Cedex 05, France*

[b] *Centro de Física Nuclear, Universidade de Lisboa, 1649-003 Lisbon, Portugal*

[c] *CEA/Saclay, DAPNIA, 91191 Gif-sur-Yvette Cedex, France*

The MICROMEGAS detector concept, generally optimized for use in accelerator experiments, displays a peculiar combination of features that can be advantageous in several astroparticle and neutrino physics applications. Their sub-keV ionization energy threshold, excellent energy and space resolution, and a simplicity of design that allows the use of radioclean materials in their construction are some of these characteristics. We envision tackling experimental challenges such as the measurement of neutral-current neutrino-nucleus coherent scattering or Weakly Interacting Massive Particle (WIMP) detectors with directional sensitivity. The large physics potential of a compact (total volume O(1)m^3), multi-purpose array of low-background MICROMEGAS is made evident.

`Presented at IMAGING 2000, Stockholm, June 2000`

1. MICROMEGAS operating principle.

MICROMEGAS (MICROMEsh GAseous Structure, μMS here) is a two-stage parallel-plate avalanche chamber design consisting of a 100 μm narrow amplification gap and a thick (up to several cm) conversion region, separated by a gauze-light electroformed conducting micromesh. Electrons released in the gas-filled conversion gap by an ionizing particle are drifted to the amplification gap where they are multiplied in an avalanche process. Detectable signals are then induced on anode elements (strips or pads). These provide an accurate monodimensional or x-y spatial projection of the energy deposition. The distance between the micromesh (cathode) grid and the anode plane is maintained by spacers 150 μm in diameter, placed every ~1 mm. These are printed on a thin substrate by conventional lithography of a photoresistive polyamide film. The anode plane is similarly printed on a thin epoxy or Kapton foil. Further details of the μMS design can be found in [1–4]. As a result of their extreme rate capability (~10^6 particles mm^{-2} s^{-1}) and space resolution of O(10) μm, these devices have an obvious utility in high energy physics as tracking chambers or in medical X-ray imaging. Here we concentrate on the alternative possibility of exploiting some of the features specific to the μMS in a different realm, that of searches for rare-events in neutrino and astroparticle physics.

2. Detector features of interest.

A common denominator to the applications proposed here is the need to extrude a sporadic signal from a mound of competing backgrounds. Several properties of μMS work together toward this goal:

• Their excellent spatial resolution, presently down to 10-60 μm (depending on gas) for drift lengths of 3 mm at 1 bar [4], allows for precise particle identification based on range vs. energy considerations. The intrinsic time resolution of the detector is below 1 ns and therefore an accurate third dimension can be extracted from time

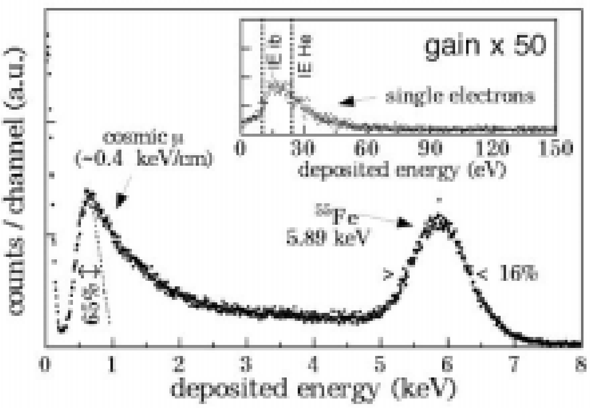

FIG. 1. Response of an unshielded He + 10% iC_4H_{10} μMS chamber ($10\times10\times1.5$ cm^3 conversion volume) to a weak ^{55}Fe source at 1 bar. The assymetry in the atmospheric muon peak is due to their $\cos^2\theta$ distribution around the zenith angle (the chamber was placed horizontally flat). *Inset:* Blow-up of the threshold region: the peak at $\sim$20 eV is mainly due to single-electron field emission from the nickel micromesh. The frequency of this process (here 10^{-2} Hz) strongly depends on operating conditions and was not optimized during this run. Ionization energies for isobutane and He are indicated, evidencing the good linearity of the device.

measurements, allowing for complete track reconstruction when necessary.

• Very often the signal sought falls in the keV or sub-keV energy region, as is the case in solar axion or WIMP searches. The high gains (up to 10^5-10^6) obtained with these chambers permit to detect single electrons with $\sim$ 100% efficiency even at elevated (20 bar) pressures [5,6]. This translates into an effective energy threshold close to the ionization energy of the gas, i.e., few tens of electronvolts (Fig. 1). Having been conceived as a TPC detector, μMS is compatible with large drift volumes and operation at high pressure, an example of which are the HELLAZ prototypes [6]. Large μMS detectors (40 cm $\times$ 40 cm $\times$ 3 mm) are presently in use [7]. A modular design providing the required performance specifications for the searches discussed here and a total target mass of several kg within a compact O(1)m^3 volume is feasible using standard μMS technology. Until now, the combination of substantial target mass (an obvious must in rare-event searches) and sub-keV energy threshold constituted a void in detector technology.

• A typical μMS energy resolution already approaches that of conventional semiconductor detectors in this low energy region, a remarkable feat for gas devices. A 5.4% keV FWHM at 22 keV has been recently obtained [8] (Fig. 2). This is required for positive identification of signals that extend over just a few keV.

• A large variety of target gas mixtures is available (He, Ne, Ar, Xe, CF_4, etc.) and compatible with high gain operation. This versatility in atomic mass and gas

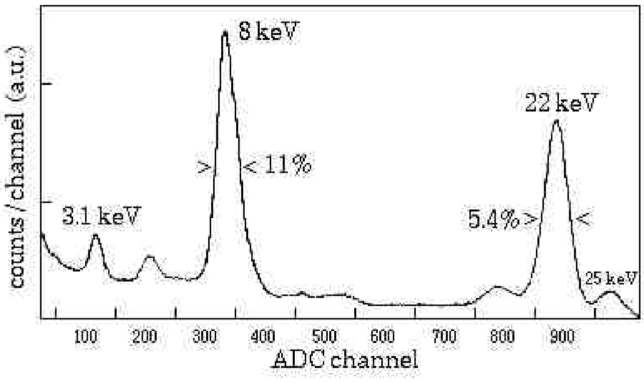

FIG. 2. Response of an Ar + 10% iC_4H_{10} μMS chamber to ^{109}Cd X-rays at 1 bar. The energy resolution is already comparable to that of large Germanium detectors.

density can be used for signal and/or background characterization. For instance, the ultimate limitation to WIMP searches is the background due to nuclear recoils from neutron scattering [9], identical to those expected from WIMP interactions. However, the dependence on target nucleus differs in both cases.

• The structural simplicity and ease of assembly of these chambers allows to manufacture them out of radioclean materials without much ado. The only components essential to the μMS design are all in the form of very thin foils, with a large freedom in the choice of building materials. Besides, intrinsic backgrounds such as spurious pulses, common in other high-gain gas detectors such as the Multi-Wire Proportional Chamber (MWPC), are absent in the μMS.

• Last but not least, their fabrication cost is low enough ($\sim$1 USD/cm^2) to envision moderate budgets for the projects discussed next.

3. Applications.

3.1 Solar axion searches.

The axion, an as-of-yet hypothetical particle arising from the Peccei-Quinn broken symmetry [10], has been the object of an extensive theoretical and experimental activity [11]. If axions exist, they can play an important role in stellar dynamics. This has prompted several searches for axion emission from our Sun [11]. Their energy spectrum, a reflection of the inner solar temperature, is expected to peak in the few keV region, dying off at $\sim$10 keV. A recently approved experiment [12] at CERN aims to revisit the "axion helioscope" approach, where an attempt is made to convert solar axions to detectable low-energy photons by use of a strong magnetic field, provided there with unprecedented intensity by a decommissioned LHC test magnet. This experiment will be performed above ground due to the large size of the cryogenic magnet. As a result, background rejection will be essential in achieving the intended sensitivity. The use of μMS chambers can largely reduce the expected background [13] which in this case will mostly consist of minimum ionizing particles leaving partial energy depositions in the spectral region of interest but having ranges that are too long to originate from an axion-induced photoelectron, or neutron-induced recoils of similar energies having ranges that are too short. The low energy threshold will allow to resolve the full axion spectrum, which in some models can peak at energies as low as 0.8 keV. Large μMS of a dimension adequate for this search ($\sim$ 10 cm drift length) have been tested [14] and prototypes built with radioclean materials are under construction. Other projects discussed in this section should profit from this R&D.

3.2 Coherent neutral-current neutrino-nucleus scattering.

An uncontroversial process in the Standard Model, the scattering off nuclei of low-energy neutrinos ($<$ few tens of MeV) via the neutral current [15] remains undetected. The long neutrino wavelength probes the entire nucleus, giving rise to a large coherent enhancement in the cross section, proportional to neutron number squared [16]. A quantum-mechanical condition for the appearance of coherent effects is the indistinguishability of initial and final states and hence the absence of a charged-current equivalent. In principle, it would be possible to speak of *portable* neutrino detectors since the expected rates can be as high as several hundred recoils/kg/day (table 1), by no means a "rare-event" situation. However, the recoil energy transferred to the target is of a few keV at most for the lightest nuclei (Fig. 3). Of this, only a few percent goes into ionization, most of it being lost as phonons. This ionization energy is generally referred to as "electron equivalent energy" (e.e.e.) and its fraction of the total as "quenching factor".

The interest in observing this process is not merely academic: a neutral-current detector responds the same way to all know neutrino types. Therefore, the observation of neutrino oscillations in such a device would be direct evidence for a fourth sterile neutrino. These must be invoked if all recently observed neutrino anomalies are accepted at face value [17] and may play an important role as dark matter [18]. Separately, the cross section for this process is critically dependent on neutrino magnetic moment: concordance with the Standard Model prediction would *per se* largely improve the present experimental sensitivity [19]. Finally, this coherent mechanism plays a most important role in neutrino dynamics in supernovae and neutron stars [15], adding to the attraction of a laboratory measurement.

Several proposals to use phonon-sensitive new-generation cryogenic detectors [20,21] have been put forward, but no existing device meets the mass and energy threshold requirements involved in this measurement. The advent of the μMS concept may have broken this impasse: Fig. 3 shows the signal expected in a

TABLE I. Expected number of neutral-current nuclear recoils in several MICROMEGAS gases from a typical reactor neutrino flux and spectrum ($10^{13}\nu$ cm^{-2} s^{-1}).

Gas	Recoils / kg / day	of which E_{rec} <1 keV	of which E_{rec} <100 eV
He	8.1	3.5	0.6
Ne	43.9	37.0	10.7
Ar	103.2	98.1	39.8
Xe	389.7	389.1	274.1

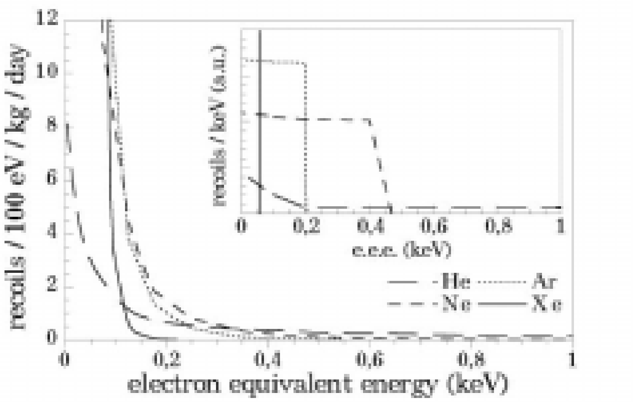

FIG. 3. Detectable signal in different MICROMEGAS gases from neutral-current nuclear scattering of reactor neutrinos ($10^{13}\nu$ cm^{-2} s^{-1}), obtained by folding of the differential cross section in [16] with the simplified reactor spectrum of [25] and applying quenching factors from [22]. The tradeoff between endpoint energy and rate with increasing atomic mass is evident. The instrumental resolution smear is not included (this should spill the signal toward higher e.e.e.'s). *Inset*: Similar signal expected from a high-purity filtered (Fe+Al) neutron beam of 24 keV (2 keV FWHM). Other available energies are 2 keV (Sc+Ti), 55 keV (Si+S) and 144 keV (Si+Ti).

reactor experiment for several gases used in μMS. A considerable fraction of the signal is found in all cases above the achieved μMS thresholds. Experimental quenching factors are nevertheless *terra incognita* at these low energies (here they have been extrapolated below 1 keV recoil energy from SRIM stopping power tables [22]). It is therefore imperative to perform preliminary measurements with a well-characterized radiation source able to produce *exclusively* these low-energy recoils. Adequate monochromatic (filtered) neutron beams [23] with negligible photon contamination are available from a handful of research reactors. The expected recoil signal falls in the same energy region as for reactor neutrinos (Fig. 3, inset). These preliminary proof-of-principle measurements could be performed immediately with the HELLAZ prototype chamber [24]. Indeed, this large-volume (25 l), high-pressure (20 bar) μMS prototype seems ready for a first-ever measurement of this interesting mode of neutrino interaction.

3.3 Weakly Interacting Massive Particles.

WIMPs constitute one of the best candidates for Dark Matter at the galactic level [26]. Numerous ongoing and planned searches aim at the detection of keV nuclear recoils induced by WIMP elastic scattering [27]. The difficulty there is the scarce number of interactions expected (<1-10 recoils/kg target mass/day) and hence the need for background reduction and/or rejection. Besides, the WIMP signal monotonically decreases with increasing energy, favoring the lowest possible detector threshold. The advantage of gas detectors with good space resolution was recognized early on [28]; nuclear recoils can be distinguished from competing backgrounds by their much shorter trajectories (Fig. 4), with near perfect rejection ability. Unfortunately, the few prototypes built so far [29,30] (based on a MWPC design) are limited by modest spatial resolutions of O(1)mm, the possibility of spurious pulses at low energies and the need to operate at reduced pressure to obtain a particle identification ability in the keV region. As a result of the last, their volume-to-target mass is less than optimal (multi-m^3/kg) in view of the low signal rate expected. The radically superior space resolution of μMS can overcome this setback, reverting this ratio (multi-kg/m^3). Other advantages can be listed:

• High-spatial resolution gaseous detectors can determine the initial direction of a recoiling nucleus. The Sun's movement through the galactic halo produces a pseudo-collimation of the WIMP flux, which in turn engenders an anisotropy in recoil direction [31]. This gives rise to a wickedly complex, geographically-dependent WIMP signature. Not only this anisotropy changes with a diurnal periodicity due to the Earth's rotation, but it goes out of phase yearly (due the Earth's orbital motion). Its observation would constitute a far more convincing evidence for WIMP dark matter than the so-called "annual modulation", in face of a number of seasonal effects able to mimic the last.

• Fluorine is the best target for the detection of spin-dependent WIMP interactions [32]. Modest-mass CF_4-filled μMS can explore a substantial fraction of supersymmetric WIMP parameter space beyond the reach of the most ambitious cryogenic proposals [33]. Xe loading of the same device would be optimal for spin-independent (coherent) interactions due to its large nuclear mass.

• A putative population of solar-bound WIMPs, gravitationally captured via several plausible mechanisms is only within reach of detectors having sub-keV ionization thresholds [34]. Again, the combination of mass and threshold requirements has made this search impossible until now.

• The competitiveness of compact, direction-sensitive gaseous WIMP detectors with respect to tonne or multi-tonne solid-state devices has been emphasized before [30].

4. Conclusions

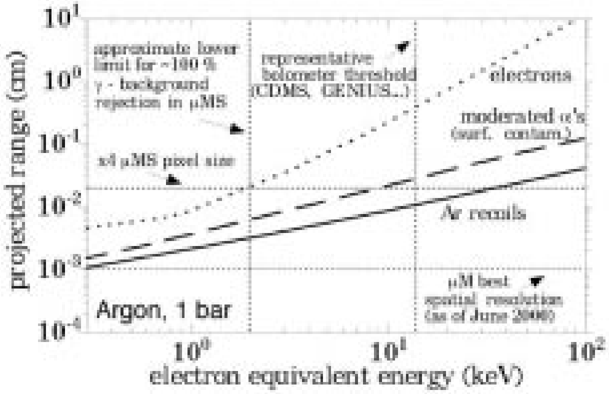

FIG. 4. WIMP-induced nuclear recoils can be efficiently separated from competing backgrounds in gas detectors due to their shorter ranges. In the case of μMS, the small pixel size will permit a $\sim$ 100% background rejection down to unprecedented low-energies (detailed calculations for a variety of gases and pressures are in progress).

The feasibility of other applications is still under study. For instance, in beta-decay kinematic tests for neutrino mass, the achievable sensitivity depends similarly on source intensity and energy resolution of the spectrometer. The fast response of a tritium-spiked μMS may allow to use (before pile-up constrains become an issue) a decay rate amply able to compensate for a diminished energy resolution vis-a-vis dedicated spectrometers. An alluring possibility is the "miniaturization" of neutrino oscillation experiments by use of a compact-yet-intense ^{3}H source like that described in [36], surrounded by a small array of μMS chambers. The reachable $\overline{\nu}_e \rightarrow \nu_x$ parameter space is largely unexplored and may, for a large enough source, extend to the region favored to explain the solar neutrino deficit. The same set-up could be used simultaneously for conventional neutrino magnetic moment searches [37], where a departure from the Standard Model prediction in the low-energy antineutrino-electron scattering cross section is looked for. The neutrino flux from such a source can be a factor >100 larger than in reactors but the maximum electron recoil energy is ~1 keV, again severely constraining the choice of detector [38].

All in all, we foresee a busy future for MICROMEGAS in the field of low-background, low-energy experiments.

5. Acknowledgments:

We are indebted to J. Derre and P. Gorodetzky for many useful discussions and suggestions.

---

[1] Y. Giomataris, Ph. Rebourgeard, J.P. Robert, and G. Charpak, Nucl. Instr. Meth. **A376**, 29 (1996).

[2] Y. Giomataris, Nucl. Instr. Meth. **A419**, 239 (1998).
[3] J.P. Cussonneau *et al.*, Nucl. Instr. Meth. **A419**, 452 (1998).
[4] J.Derre *et al.*, DAPNIA/00-3, subm. to Nucl. Instr. Meth.
[5] J. Derre *et al.*, Nucl. Instr. Meth. **A449**, 314 (2000).
[6] P. Gorodetzky *et al.*, Nucl. Instr. Meth. **A433**, 554 (1999); P. Gorodetzky *et al.*, these proceedings.
[7] D. Thers *et al.*, DAPNIA/SPHN-00-35, submitted to Nucl. Instr. Meth.
[8] A. Delbart *et al.*, DAPNIA/SED-00-01, submitted to Nucl. Instr. Meth.
[9] P. Di Stefano *et al.*, `astro-ph/0004308`
[10] R.D. peccei and H. Quinn, Phys. Rev. Lett. **38**, 1440 (1977) ; S. Weinberg, Phys. Rev. Lett. **40**, 223 (1978) ; F. Wilczek, Phys. Rev. Lett. **40**, 279 (1978).
[11] L. J. Rosenberg and K. A. van Bibber, Phys. Rep. **325**, 1 (2000).
[12] C. E. Aalseth *et al.*, Nucl. Instr. Meth. **425**, 482 (1999) ; `http://collar.home.cern.ch/collar/SATAN/alvaro.html`; `http://axnd02.cern.ch/CAST/`
[13] `http://collar.home.cern.ch/collar/SATAN/TRANSP/bckgrejection(14).doc` ; *ibid*, `bckgconcl(15).doc`
[14] *ibid* [13], `Ar_response(12).doc` and `fe55irrad(13).doc`
[15] D. Z. Freedman *et al.*, Annu. Rev. Nucl. Sci. **27**, 167 (1977).
[16] A. Drukier and L. Stodolsky, Phys. Rev. **D30**, 2295 (1984).
[17] J. Ellis, proc. of NEUTRINO 2000 (`hep-ph/0008334`).
[18] A.D. Dolgov and S.H. Hansen, `hep-ph/0009083`.
[19] A. C. Dodd *et al.*, Phys. Lett. **B266**, 434 (1991).
[20] B. Cabrera *et al.*, Phys. Rev. Lett. **55**, 25 (1985).
[21] A. S. Starostin and A. G. Beda, `hep-ex/0002063`.
[22] `http://www.research.ibm.com/ionbeams/`
[23] R. C. Block and R. M. Brugger in "Neutron Sources for Basic Physics and Applications", A. Michandon *et al.* eds., Pergamon, NY, 1983.
[24] P. Gorodetzky, private communication.
[25] F. T. Avignone, Phys. Rev. **D2**, 2609 (1970).
[26] G. Jungman *et al.*, Phys. Rept. **267**, 195 (1996).
[27] For an update, see contributions of D. Akerib and V. Zacek to NEUTRINO 2000, available from `http://nu2000.sno.laurentian.ca/June20.html`
[28] J. Rich and M. Spiro, DphPE-88-04 ; G. Gerbier *et al.*, Nucl. Phys. (Proc. Suppl.) **B13**, 207 (1990).
[29] K. Buckland *et al.*, Phys. Rev. Lett. **73**, 1067 (1994).
[30] D. P. Snowden-Ifft *et al.*, Phys. Rev. **D61**, 101301(R) (2000); C. J. Martoff *et al.*, procs. of the *2nd Intl. Workshop on the Identification of Dark Matter (IDM98)*, World Scientific, Singapore, 1999, p. 389.
[31] D. N. Spergel, Phys. Rev. **D37**, 1353 (1988).
[32] J. Ellis and R.A. Flores, Phys. Lett. **B263**, 259 (1991).
[33] J. I. Collar *et al.*, New J. of Physics **2**, 14.1 (2000).
[34] Reviewed in: J. I. Collar, Phys. Rev. **D59**, 063514 (1999).
[35] E. Cosulich *et al.*, Phys. Lett. **B295**, 143 (1992).
[36] V. N. Trofimov *et al.*, Yad. Fiz. **61**, 1373 (1998).
[37] A. Tadsen *et al.*, Nucl. Phys. (Proc. Suppl.) **B78**, 131 (1999).
[38] B. S. Neganov *et al.*, J. Low Temp. Phys. **93**, 745 (1993).